



SINGLE-PHASE HIGH STEP-UP CONVERTER WITH HALF-BRIDGE-BASED PV INVERTER SYSTEM

Kannan N[#] Dr.S.Sutha[@] and B. Nandhini^{*}

[#]Research Scholar, EEE, Anna University, Chennai, India

[@]Assistant Professor, EEE, University Collee of Engineering, Dindugal, India

^{*}(B.E),EEE, University College of Engineering, Ariyalur,

Abstract-In this paper, a single-phase high step-up converter is proposed, designed not only to boost the relatively low photovoltaic (PV) voltage to a high bus voltage with high efficiency, but also to offer a neutral point terminal for the half-bridge-based inverters. First and foremost, two symmetrical high step-up converters are combined and integrated to derive an improved converter with neutral point terminal, which is strongly expected for the half-bridge-based inverters. Secondly, the voltage gain of the converter is extended and the narrow turn-off period is avoided by using the coupled inductor multiplier. Furthermore, the coupled inductor multiplier reduces the voltage stress of all the power devices. As a result, the low voltage-rated power devices can be employed to minimize the conduction losses. More importantly, all the active switches work in the zero-voltage-switching condition, which reduces the switching losses effectively. All these factors improve the circuit performance in the high step-up applications, especially for the half-bridge based PV inverter systems. Finally, the experimental results from a 500 W, 48–760 V prototype at 100 kHz switching frequency are provided to verify the effectiveness of the proposed converter. The highest efficiency of the prototype is 96.5% and the efficiency is over 94% in a wide load range.

1. INTRODUCTION

Because of the environmental problems on the global warming and the increasing threat of the fast exhaustion of the fossil fuel, more and more efforts have been made to explore the renewable energy sources, such as the wind generation, the geothermal, the photovoltaic (PV), and the fuel cells. These renewable energy sources can generate electricity without harming the environment. In recent years, as one of the most promising sources in the renewable energy, the distributed PV generation systems have received increasing popularity in the residential areas. Therefore, many researchers concentrate on the small size PV grid-connected inverter, which is desired for the low-power and high-efficiency applications.

In the low power grid-connected PV system, the transformer less configuration has become a widespread tendency due to its higher efficiency, smaller size, lighter weight, and lower cost compared with the isolated counterparts. However, in the transformerless condition, when the traditional full bridge inverter with unipolar sinusoidal pulse width modulation (SPWM) modulation is adopted, the common mode (CM) ground leakage current may appear on the parasitic capacitor between the PV cell and the ground, which brings out the safety issue and reduces the efficiency of the inverter. Consequently, how to suppress and eliminate the CM leakage current

caused by the parasitic capacitor between the PV and the ground is one of the most emergent technologies. Unfortunately, some published state-of-the-art full-bridge-based transformer less inverters, such as H5 inverter, H6 inverter, the HERIC inverter and so on, contain more power switches or increase the conduction losses. In fact, the half-bridge inverter and neutral point clamped (NPC) inverter can naturally eliminate the CM leakage current because the grid neutral line is directly connected to the neutral point of the dc bus. However, the dc bus voltage of the half-bridge-based inverters should be twice as that of the full-bridge-based topologies and the neutral point of the dc bus should be also required. Therefore, how to explore the high-step-up and high-efficiency dc-dc converters is nowadays the focus of an intensive research effort by the power electronics community. These high step-up converters are strongly expected to not only boost the relatively low voltage to a high bus voltage with high efficiency, but also offer a neutral point terminal for the half-bridge-based transformerless inverters, which is shown in Fig 1.

The conventional boost converters are not suitable for the high step-up conversion applications because the duty cycle of the conventional boost converter with high step-up conversion is very large, which results in narrow turn-off period, large current ripple, and high switching losses. In order to achieve large voltage conversion ratio, some switched capacitor-based converters were published. With the switched capacitor technology, the conversion ratio of the converter is increased and the voltage stresses of the devices are decreased. Unfortunately, the switched capacitor technique makes the switch suffer high transient current and large conduction losses. Moreover, many switched capacitor stages are required to achieve the high voltage gain, which makes the circuit complex. It is easier for the isolated converters to achieve an extremely high voltage gain because the turn's ratio of the transformer can be employed as another control freedom to extend the voltage gain. By adjusting the transformer turns ratio appropriately, high voltage conversion ratio can be realized with optimal duty cycle. However, one inductor and one transformer are necessary in these converters, which increase the circuit volume and reduce the power density. Furthermore, the driving circuits and the sampling circuits in the isolated converters may increase the system complexity when compared with those in the non-isolated converters. Christo Ananth et al. [2] discussed about principles of Electronic Devices which forms the basis of the project.

In fact, most of the non-isolated high step-up converters can be derived from their isolated counterparts. Some high step-up boost converters with coupled inductor are introduced to achieve large voltage conversion ratio.

The voltage gain is extended and the switch voltage stress is reduced by the transformer function of the coupled inductor. Moreover, only one magnetic component is used, which reduces the volume and the complexity of the converter. However, the leakage inductance of the coupled inductor may not only bring about high voltage spikes on the switch when it turns OFF, but also induce large energy losses. Combining the concept of coupled inductor and switched capacitor, a single-phase improved active clamp-coupled inductor-based converter with extended voltage doubler cell is proposed with some significantly indispensable advantages, such as voltage gain extension without extreme duty-cycle, switch voltage stress reduction, zero-voltage-switching (ZVS) soft switching operation and output diode reverse-recovery problem alleviation. Unfortunately, this converter cannot offer a neutral point terminal for the half-bridge-based transformer less inverters. However, it provides an excellent high step-up converter candidate for further topology derivation if the neutral point terminal is required.

In this paper, an improved single-phase high step-up converter with coupled inductor multiplier is derived, which has all the above-mentioned advantages that the converter in has Active inductor coupled based converter. More importantly, the proposed converter can naturally create a neutral point terminal and its voltage gain is twice of that of the converter in Active inductor coupled based converter, which can be employed as a high step-up dc-dc converter for the secondary half-bridge-based transformerless inverter system. The topology derivation principle is highlighted and the circuit operation of the proposed converter is explored clearly. The advantageous circuit performance can be proved by a 500-W 48-760 V prototype operating at 100-kHz switching frequency.

1. BLOCK DIAGRAM:

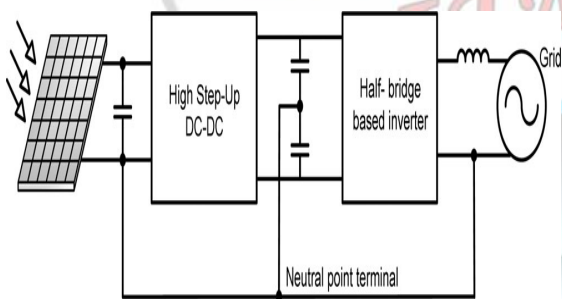


Fig.1.High step-up dc-dc converter for half-bridge-based inverter.

PHOTOVOLTAIC CELL:

PV cells are made of semiconductor materials, such as silicon. For solar cells, a thin semiconductor wafer is specially treated to form an electric field, positive on one side and negative on the other. When light energy strikes the solar cell, electrons are knocked loose from the atoms in the semiconductor material. If electrical conductors are attached to the positive and negative sides, forming an electrical circuit, the electrons can be captured in the form of an electric current - that is, electricity. This electricity can then be used to power a load. A PV cell can either be circular or square in construction

DC-DC CONVERTERS:

DC-DC converters can be used as switching mode regulators to convert an unregulated dc voltage to a regulated dc output voltage. The regulation is normally achieved by PWM at a fixed frequency and the switching device is generally BJT, MOSFET or IGBT. The minimum oscillator frequency should be about 100 times longer than the transistor switching time to maximize efficiency. This limitation is due to the switching loss in the transistor. The transistor switching loss increases with the switching frequency and thereby, the efficiency decreases. The core loss of the inductors limits the high frequency operation. There are four topologies for the switching regulators: buck converter, boost converter, buck-boost converter, cirkconverter. However my paper work deals with the boost regulator and further discussions will be concentrated towards this one.

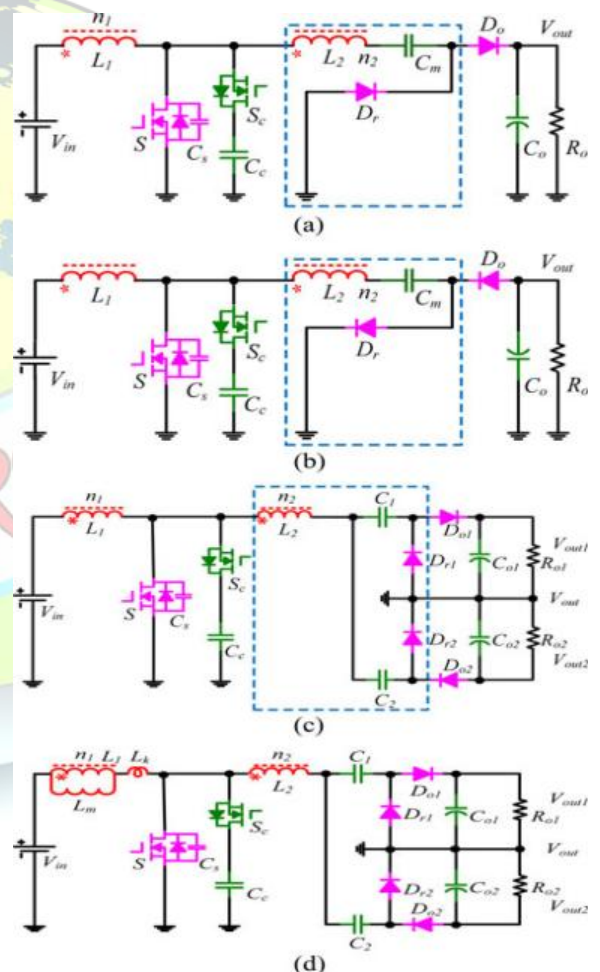


Fig. 2.Topology derivation: (a) active clamp-coupled inductor-based converter; (b) symmetrical converter based on the converter in [active clamp coupled-Inductor-based converter];(c) Proposed converter; (d) equivalent converter.

HALF BRIDGE INVERTER

The D.C to A.C power converters are known as inverters. An inverter is a circuit which converts a D.C power into A.C power at desired output voltage and frequency. The A.C output voltage could be fixed at a fixed or variable frequency. Switches S_1 and S_2 are the gate commutated devices such as power BJTs, MOSFETs, GTO, IGBT, MCT, etc. Switch S_1 Conducting time period ($0 < t < T/2$) and Switch S_2 Conducting time period ($T/2 < t < T$), $T=1/f$ and f is the frequency of the output voltage waveform.

3. CIRCUIT OPERATIONAL ANALYSIS

The single-phase coupled-inductor-based converter with extended voltage doubler cell proposed in Single-phase improved active clamp coupled-inductor-based converter with extended voltage doubler cell is given in Fig. 2(a). The extended voltage doubler cell circuit is plotted in the dash block, composed by an inductor L_2 , a switched capacitor C_m , and a regenerative diode D_r . The clamp circuit is composed of an auxiliary switch S_c and a capacitor C_c . Based on the converter in Single-phase improved active clamp coupled-inductor-based converter with extended voltage doubler cell, a symmetrical converter shown in Fig. 2(b) can be easily derived by changing the direction of regenerative diode

D_r , output diode D_o , and output capacitor C_o . Compared with the converter in Single-phase improved active clamp coupled-inductor-based converter with extended voltage doubler cell, the converter in Fig. 2(b) operates similarly and offers a negative output voltage. More importantly, the converter in Fig. 2(b) has the same active switches and coupled inductance with the converter in Fig. 2(a). Therefore, by combining and integrating these two symmetrical converters, the proposed converter can be derived without adding extra active switches and magnetic component, which is given in Fig. 2(c).

In the proposed converter, the clamp circuit includes a switch S_c and a capacitor C_c . The coupled inductor multiplier in the dash block contains a secondary winding of the coupled inductor, two switched capacitors C_1 and C_2 , and two regenerative diodes $D_r 1$ and $D_r 2$. The inductor L_1 is coupled to the inductor L_2 . The coupling reference is marked by "*", and the turns ratios is expressed by $N = n_2 / n_1$. The output load can be divided into two equal parts, the voltage on the load R_{o1} is V_{out1} and the voltage on the load R_{o2} is V_{out2} .

The coupled inductor can be considered as an ideal transformer, a parallel magnetizing inductance and a series leakage inductance. High-efficiency, high step-up DC-DC converters. The equivalent circuit of the proposed converter is shown in Fig. 2(d). L_1 and L_2 represent the primary and secondary windings, respectively. C_s is the parallel capacitor, including the parasitic capacitors of the main and clamp switches.

As shown in Fig. 3, there are eight main operation stages in one switching cycle. The explanation of the key

waveforms is the following: i_{Lk} is the current through the leakage inductance L_k ; v_{ds} is the voltage across the main switch S ; v_{C_c} is the voltage across the clamp capacitor C_c ; i_{C_c} is the current through the clamp circuit S_c and C_c ; i_{L_2} is the current through the secondary winding L_2 ; $v_{D_{o1}}$, $v_{D_{r1}}$, $v_{D_{o2}}$, $v_{D_{r2}}$, and $i_{D_{o1}}$, $i_{D_{r1}}$, $i_{D_{o2}}$, and $i_{D_{r2}}$ are the voltages and currents of the diodes D_{o1} , D_{r1} , D_{o2} , and D_{r2} . The equivalent circuits for each stage are shown in Fig. 4.

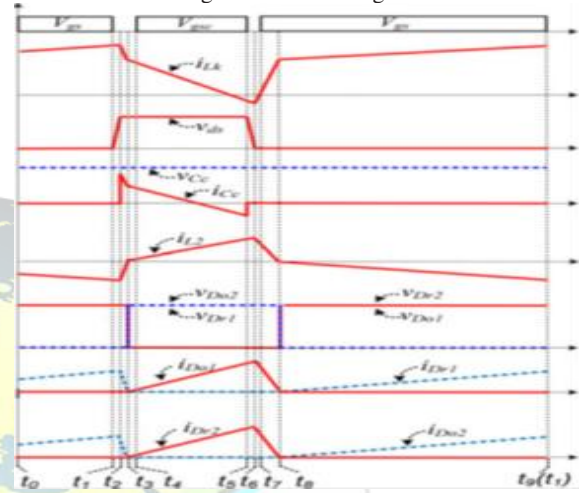


Fig. 3. Key waveforms of converter.

Stage 1 [$t_0 - t_1$]: Before t_1 , the main switch S is in the ON state, while the clamp switch S_c is in the OFF state. During this period, the diodes D_{r1} and D_{o2} conduct, while D_{o1} and D_{r2} are reverse biased.

The magnetizing inductance L_m and the leakage inductance L_k are charged by the input voltage V_{in} ; thus, the magnetizing current and leakage inductance current increase gradually almost in a linear way. At the same time, the switched capacitor C_1 is charged by the secondary winding L_2 , also the energy stored in L_2 and the switched capacitor C_2 is transferred to the load R_{o2} .

Stage 2 [$t_1 - t_2$]: The main switch S turns OFF at t_1 , then the parallel capacitor C_s begins to resonate with the leakage inductance L_k . Considering that C_s is small and L_k is relatively large, the voltage v_{ds} on the main switch S rises almost at a constant slope from zero. The turn-off losses of the main switch are reduced due to the existence of C_s .

Stage 3 [$t_2 - t_3$]: At t_2 , the switching voltage of the main switch reaches the clamp capacitor voltage, and the antiparallel diode of the clamp switch S_c conducts. Then v_{ds} is clamped to v_{C_c} by the antiparallel diode of the clamp switch S_c . Since the clamp capacitor C_c is much larger than C_s , C_s can be neglected and almost all the current flow through C_c . After t_2 , the leakage inductance L_k is discharged by the voltage of C_c . In this stage, the current through L_k decreases sharply, as well as the current through the secondary winding.



Stage 4 [$t_3 - t_4$]: At t_3 , i_{L2} falls to zero, then the diodes Do1 and Dr 2 begin to conduct, while Dr 1 and Do2 are reverse bi-

ased. In this stage, both Lm and Lk are discharged; thus, the current through Lk decreases gently when compared to Stage

3. At the same time, the switched capacitor C2 is charged by the secondary winding L2, also the energy stored in L2 and the switched capacitor C1 is transferred to the load Ro1.

Stage 5 [$t_4 - t_5$]: The turn-on signal is applied to the clamp switch Sc at t_4 . Sc is turned ON when its body diode is conducting; thus, the ZVS turn-on condition of the clamp switch Sc is achieved. The equivalent circuit and current equations in this stage are similar to that of Stage 4.

Stage 6 [$t_5 - t_6$]: The clamp switch Sc is turned OFF at t_5 . After that the parallel capacitor Cs begins to resonant with the

leakage inductance Lk again. Because Cs is small and Lk is relatively large, voltage on the main switch vds decreases almost

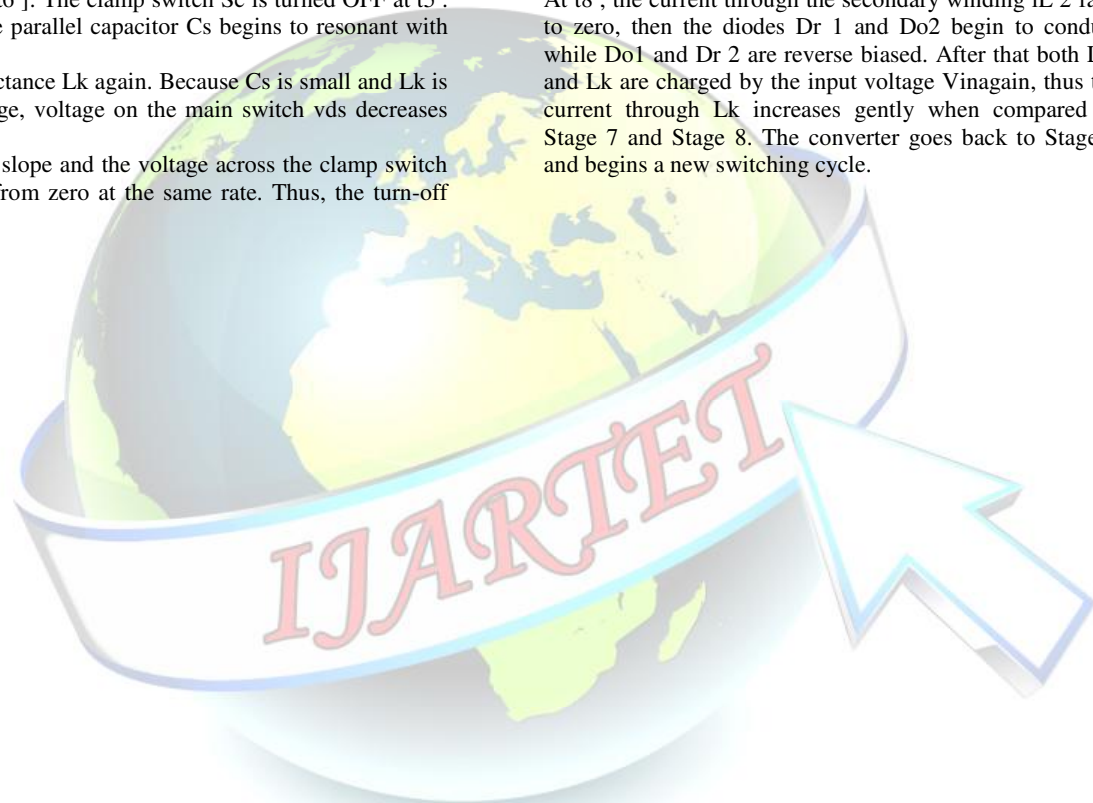
at a constant slope and the voltage across the clamp switch Sc increases from zero at the same rate. Thus, the turn-off

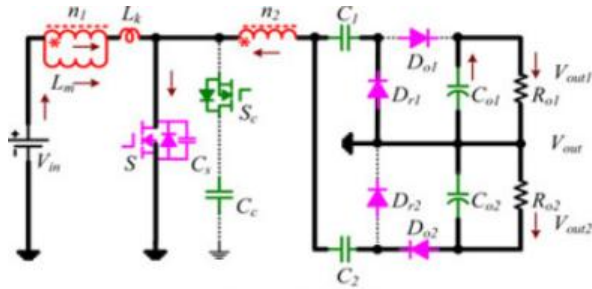
losses of the clamp switch are reduced due to the existence of Cs. The analysis in this stage is very similar to Stage 2.

Stage 7 [$t_6 - t_7$]: The voltage of the parallel capacitor Cs falls to zero at t_6 , and then the antiparallel diode of the main switch S begins to conduct. Cs and Lk stop resonating. The increasing rate of the current through Lk is controlled by the output voltage, and at t_6 the current through the secondary winding i_{L2} begins to fall.

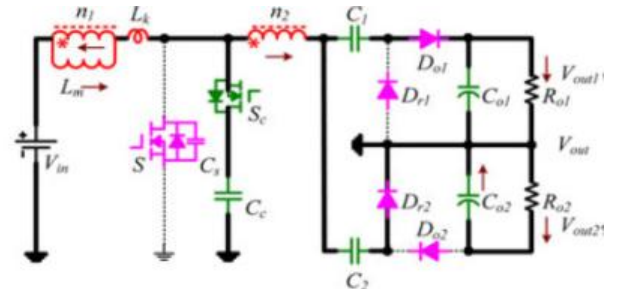
Stage 8 [$t_7 - t_8$]: The turn-on signal is applied to the main switch S when its antiparallel diode is conducting; thus, the ZVS turn-on condition of the main switch S is achieved. The equivalent circuit and current equation in this stage are similar to Stage 7.

At t_8 , the current through the secondary winding i_{L2} falls to zero, then the diodes Dr 1 and Do2 begin to conduct while Do1 and Dr 2 are reverse biased. After that both Lm and Lk are charged by the input voltage Vin again, thus the current through Lk increases gently when compared to Stage 7 and Stage 8. The converter goes back to Stage 1 and begins a new switching cycle.

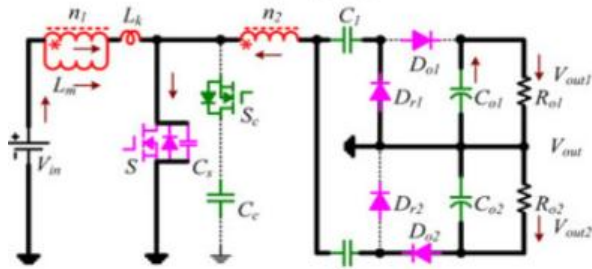




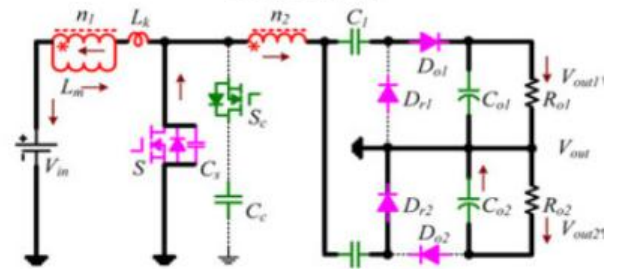
Stage 1 [$t_0 \sim t_1$]



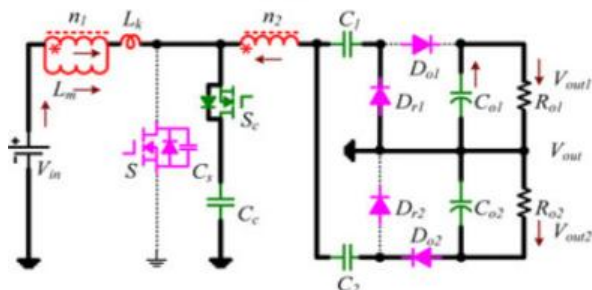
Stage 5 [$t_4 \sim t_5$]



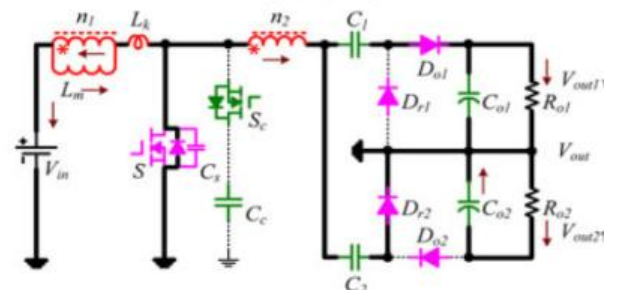
Stage 2 [$t_1 \sim t_2$]



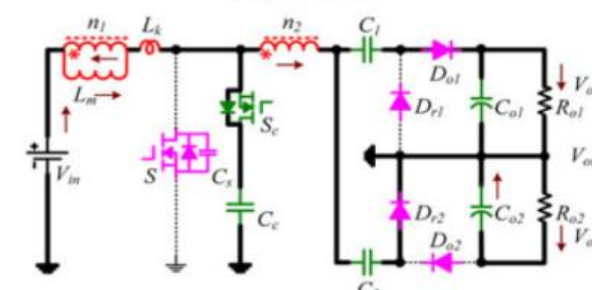
Stage 6 [$t_5 \sim t_6$]



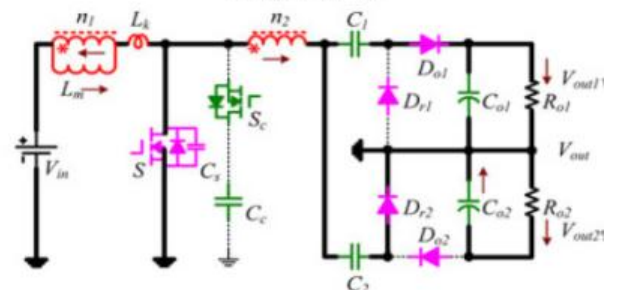
Stage 3 [$t_2 \sim t_3$]



Stage 7 [$t_6 \sim t_7$]



Stage 4 [$t_3 \sim t_4$]



Stage 8 [$t_7 \sim t_8$]

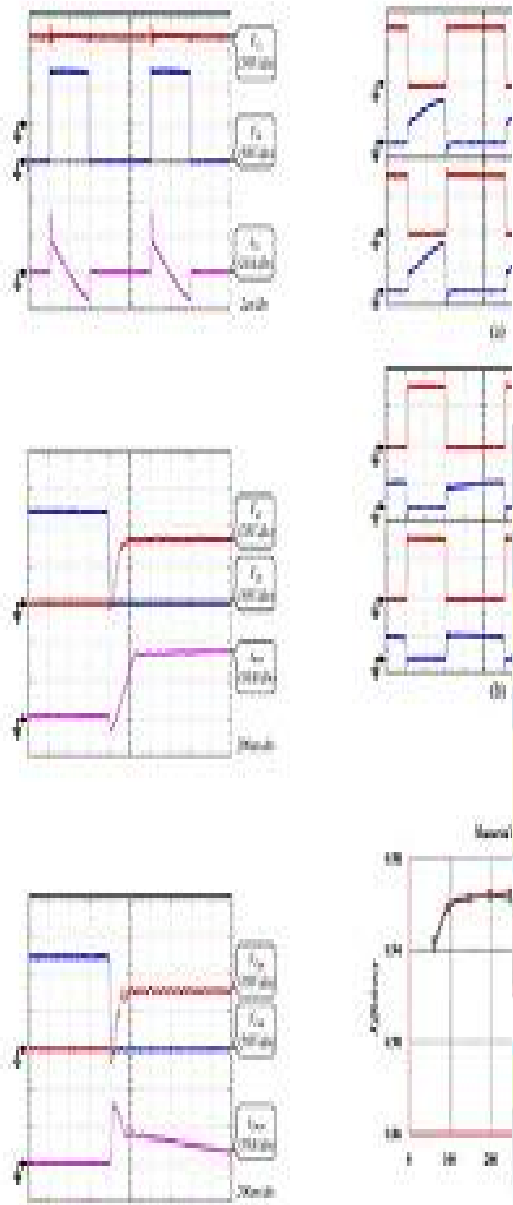


Fig:a)clamp circuit performance b)ZVS on performance of main switch c) ZVS-on performance of clamp switch

4. CONCLUSION:

The gate-source voltage, drain-source voltage, and current waveforms of the main and clamp switches are shown in Figs. 9 and 10, respectively. It can be found that ZVS turn-on conditions are realized for both the main and clamp switches during the whole switching cycle, which reduces the switching losses significantly.

The voltage and current waveforms of the four diodes are illustrated in Fig. 11. It is shown that the voltage stresses of

these four diodes are equal to half of the output voltage and the reverse-recovery problem of diodes is partly solved.

The measured efficiency of the prototype at different loads under different input voltages is sketched in Fig. 12. The highest efficiency of the converter is 96.5%, and the efficiency is higher than 94% over a wide load range.

In order to provide a neutral point terminal for the half-bridge-based inverters, this paper has proposed a single-phase high step-up converter which not only boosts the relatively low PV voltage to a high bus voltage but also offers a neutral point output voltage without any additional active switches and magnetic components. This converter presents some clear main advantages.

1) By combining and integrating two symmetrical high step-up converters, a neutral point terminal is created, which meets the input voltage requirement of the half-bridge-based inverter.

2) A coupled inductor multiplier which consists of a secondary winding of the coupled inductor, two switched capacitors and two regenerative diodes are employed in the converter to extend the voltage gain and reduce the voltage stress of the switches. So the high performance switches with low RDS-on are adopted to reduce the conduction losses and improve the efficiency.

3) The ZVS condition is achieved for all the active switches, which reduces the switching losses greatly, especially in high-frequency and high-power applications. Finally, a 500-W prototype has been built to verify the theoretical analysis and the experimental results have demonstrated that the proposed converter is a good candidate for the half-bridge-based PV inverter systems. It should be also pointed out that the input current of the proposed converter is pulsed, which has some negative influence on the input voltage source, especially in a little large power conversion applications.

6. REFERENCES

- [1] W. Li, X. Xiang, C. Li, W. Li, and X. He, "Interleaved high step-up ZVT converter with built-in transformer voltage doubler cell for distributed PV generation system," *IEEE Trans. Power Electron.*, vol. 28, no. 1, pp. 300–313, Jan. 2013.
- [2] Christo Ananth, S. Esakki Rajavel, S. Allwin Devaraj, P. Kannan. "Electronic Devices." (2014): 300.
- [3] S. V. Araujo, P. Zacharias, and R. Mallwitz, "Highly efficient single-phase transformerless inverters for grid-connected photovoltaic systems," *IEEE Trans. Ind. Electron.*, vol. 57, no. 9, pp. 3118–3128, Sep. 2010.
- [4] W. Yu, J.-S. Lai, H. Qian, C. Hutchens, J. Zhang, G. Lisi, A. Djabbari, G. Smith, and T. Hegarty, "High-efficiency inverter with H6-type configuration for photovoltaic non-isolated ac module applications," in *Proc. IEEE Appl. Power Electron. Conf.*, 2010, pp. 1056–1061.
- [5] Y. Gu, W. Li, Y. Zhao, B. Yang, C. Li, and X. He, "Transformer less inverter with virtual DC bus concept for cost-effective grid-connected PV power systems," *IEEE*



Trans. Power Electron., vol. 28, no. 2, pp. 793–804, Feb.2013.

[6] G. Roberto, L. Jesus, S. Pablo, G. Eugenio, U. Alfredo, and M. Luis, “High-efficiency transformerless single-phase photovoltaic inverter,” in Proc. IEEE EPE-PEMC, 2006, pp. 1895–1900.

[7] R. Gonzalez, E. Gubia, J. Lopez, and L. Marroyo, “Transformerless single-phase multilevel-based photovoltaic inverter,” IEEE Trans. Ind. Electron., vol. 55, no. 7, pp. 2694–2702, Jul. 2008.

[8] M. Prudente, L. L. Pfitscher, G. Emmendoerfer, E. F. Romaneli, and R. Gules, “Voltage multiplier cells applied to non-isolated DC–DC converters,” IEEE Trans. Power Electron., vol. 23, no. 2, pp. 871–887, Mar.2008.

[9] M. Nymand and M. A. E. Andersen, “High-efficiency isolated boost dc-dc converter for high-power low-voltage fuel-cell applications,” IEEE Trans.Ind.Electron., vol. 57, no. 2, pp. 505–514, Feb. 2010.

[10] Y. Zhao, W. Li, and X.He, “Single-phase improved active clamp coupled- inductor-based converter with extended voltage doubler cell,” IEEE Trans.Power Electron., vol. 27, no. 6, pp. 2869–2878, Jun. 2012.

[11] Q. Zhao and F. C. Lee, “High-efficiency, high step-up DC-DC converters,”IEEE Trans. Power Electron., vol. 18, no. 1, pp. 65–73, Jan. 2003.

[12] M. T. Zhang, Y. Jiang, F. C. Lee, and M. M. Jovanovic, “Single-phase three-level boost power factor correction converter,” in Proc. IEEE Appl. Power Electron. Conf., 1995, pp. 434–439.

[13] G. Yao, M. Ma, Y. Deng, W Li, and X.He, “An improved ZVT PWM three level boost converter for power factor preregulator,” in Proc. IEEE.Power Electron. Spec. Conf., 2007, pp. 768–772.